J. Membrane Biol. 19, 229–252 (1974)


# Model Approaches for the Evaluation of Electrical Cell Coupling in the Salivary Gland of the Larva of *Drosophila Hydei.* The Influence of Lysolecithin on the Electrical Coupling

G. E. P. M. van Venrooij, W. M. A. Hax, G. F. van Dantzig, V. Prijs and J. J. Denier van der Gon

Department of Medical Physics, Physical Laboratory, Sorbonnelaan 4, Utrecht, The Netherlands

Received 26 November 1973; revised 18 July 1974

*Summary.* In this paper, discrete as well as continuous models are developed to enable accurate interpretations of experimental findings of electrical cell coupling in the salivary gland of the larva of *Drosophila hydei.* With the help of these models it is possible to determine the nonjunctional and junctional membrane resistance as well as the confidence interval of these estimates. Apart from the easy culture of larvae and large diameters of the cells, the distal part of the salivary gland proves to be an excellent object for studying electrical cell coupling in a quantitative way. It is found that there are differences between electrical parameters in the proximal part and in the distal part of the gland. Furthermore, the value of the junctional resistance appears to be dependent on the age of the gland. Using the model descriptions, the influence of lysolecithin upon the electrical cell coupling is estimated in a quantitative way. It is demonstrated that lysolecithin, if added to the surrounding fluid, produces in a reversible way an increase in the nonjunctional permeability and a decrease in junctional permeability. No changes in membrane capacity were observed.

Cell communication may well play an important role in the processes of cell differentiation and tissue growth (Loewenstein, 1966; 1968; Furshpan & Potter, 1968). In turn, cell communication is not a stationary phenomenon but is itself controlled by a number of processes and changes during growth. Cyclic AMP (cAMP) and lysolecithin are of interest in relation to these processes. cAMP, an intermediate in the action of many hormones, has been reported to be involved in the regulation of cellular growth by inducing respectively restoring contact inhibition of cell proliferation (for references *see* companion paper, Hax *et al.*, 1974). Lysolecithin influences membrane permeability in general (van Zutphen, 1970; Reman, 1971).

For studying the effects of lysolecithin and cAMP, the salivary gland of the larva of *Drosophila hydei* was chosen because of the easy culture and the large dimensions of the gland cells (diameter up to 100 $\mu$m) resulting in an easy access for micropipettes under microscopic control. Since the gland is similar to a one-dimensional cable, responses to an electrical stimulation may be detected at relatively large distances from the source. Also its geometry permits a reliable estimate of the relevant parameters.

The glands may be subdivided into two groups according to their cell configuration. Therefore, two discrete models are considered for the quantitative estimation of junctional and nonjunctional membrane resistances following approaches similar to those of Siegenbeek van Heukelom, Denier van der Gon and Prop (1970, 1972) and Siegenbeek van Heukelom, Slaaf and van der Leun (1972). It will be shown that the differences in results of the calculations on these two models are of minor importance compared with other errors arising during the experiments.

Also a continuous model is considered in which the junctional membrane resistances are included in the intracellular fluid resistance.

The models are compared with each other, because in using these models quite different assumptions are made. The model descriptions were used for evaluating the effect of a medium containing lysolecithin on membrane properties. It was found that the permeability of the nonjunctional membranes increases in a reversible way whereas the junctional membrane permeability decreases. In the companion paper (Hax *et al.*, 1974) the results of the measurements on the influence of cAMP on the parameters of the salivary gland will be discussed.

## Materials and Methods

All experiments were performed with a wild type stock of *Drosophila hydei* cultured at 23 °C on standard nutritive medium of the same composition as given by Poels (1970).

After dissection the two salivary glands were transfered to a perspex chamber filled with a bathing fluid [modified Shields and Sang medium, described by Poels (1972)]. The transfer of the salivary glands was carried out with tweezers placed upon the duct to avoid damage of gland cells. The bottom of the perspex chamber was covered with a thin translucent Sylgard gel layer. The salivary glands were fixed to the bottom by way of a staple placed over the duct.

During the electrical measurements photographs were made of the salivary glands. These photographs were used for measuring morphological quantities, like luminal radius, gland radius and length of the gland.

### *Electrical Measurements*

The experimental set-up is shown in Fig. 1. For the electrical measurements glass micropipettes were used. They were filled with 3 M KCl and had a d-c resistance between

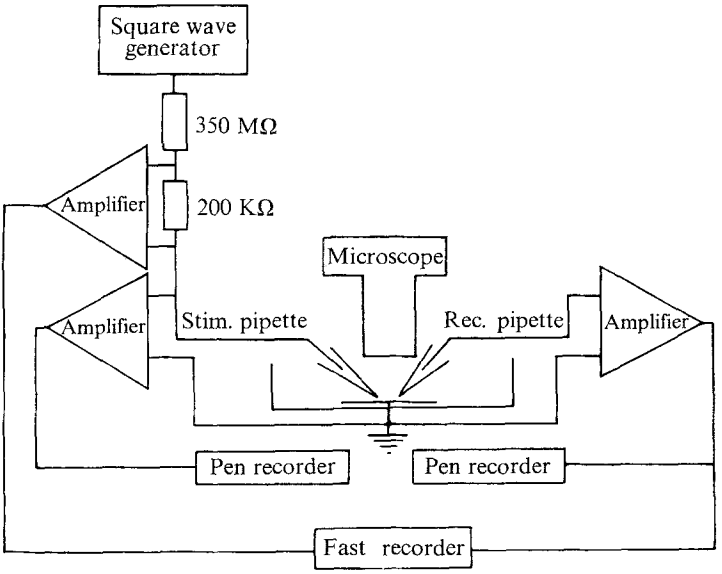


Fig. 1. Diagram of the experimental set-up

20 and 40 MΩ and a tip potential in the bathing fluid of about 2 mV. A 1-Hz symmetrical square wave with an amplitude of 10 nA was injected into the most distal cell of the salivary gland. This current was measured as a voltage drop across a resistor between the square-wave generator and the stimulating micropipette and recorded on a fast recorder (bandwidth DC-3 kHz). The second micropipette recorded the voltage changes in the gland at different distances from the stimulating micropipette. These changes were fed into a high input-impedance amplifier (input resistance higher than $10^{11}$ Ω). For accurate measurements of fast voltage changes due to the current injection the output of this amplifier was also fed into the fast recorder. Two pen-recorders (bandwidth DC-0.5 Hz) recorded the intracellular potentials as measured with the micropipettes.

The manipulations were carried out under visual control using a microscope with dark field illumination. The advantage of such a microscope is the good visualization of the cell boundaries.

All measurements were carried out within 2 hr after dissection of the glands. From experiments during which the micropipettes were held in the cells for a few hours it was found that the variation in recorded induced potential within a cell of the distal part was not more than 10% within 2 hr after dissection.

From measurements during which the same cells repeatedly were impaled, it became evident that there were no remarkable changes in recorded potentials, even when the same cells were impaled eight times. It appeared that cell damage could be observed by comparing the intracellular potential of this cell with that of fresh cells.

In no cases was the fatty tissue removed because of the possibility of damage to gland cells. This fatty tissue is attached to the gland cell with a minimum of contact. Its influence upon the electrotonic spread will be low. Also, we never detected potential changes inside the fat cells during current injection into the gland.

## Theory and Analysis

In 1965, Berendes reported observations in stained sections of glands showing that at least three types of cells are present during most of the third instar, differing in dimensions and cytoplasmic content. One type is situated around the glandular duct, one in the proximal part of the gland and the other in the distal part. We have chosen the distal part (Fig. 2) for the quantitative evaluation of the electrical cell coupling.

### *Symbols and Definitions*

$\alpha = 2 + \frac{1}{2}\frac{R_i}{R_u}$

$c_L$ = capacity of the membrane on the luminal side of the cells per unit length of gland

$c_M$ = capacity of the membrane on the basal side of the cells per unit length of gland

$c_u$ = capacity of the nonjunctional membrane per unit length of gland, defined by: $c_u = c_M + c_L$

$d$ = the length of one side of the hexagon representing the membranes on the basal side of cells with order number $n$ ($n \geqq 1$)

$\varphi$ = angle, as defined in Fig. 3*a*

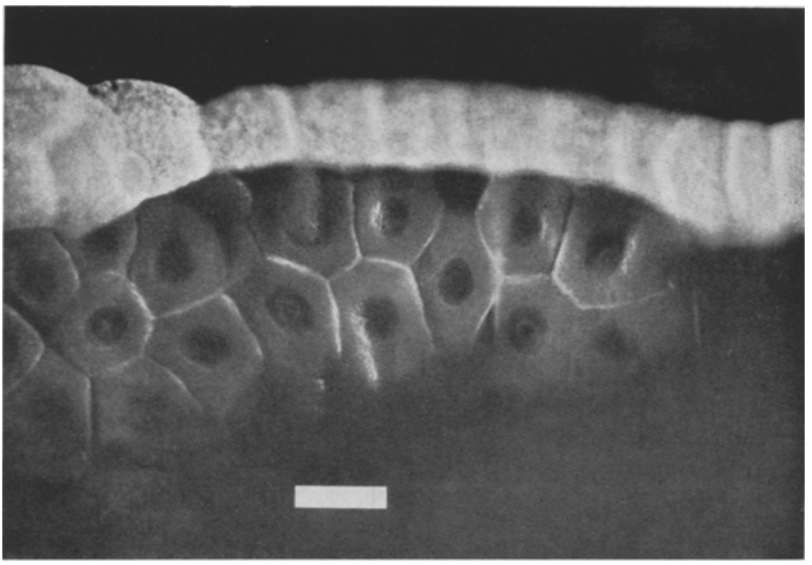

Fig. 2. Dark field view of the distal cells of the salivary gland of the larva of *Drosophila hydei* together with surrounding fat cells (bar = 100 μm)

$I$ = the injected current in the most distal cell

$\lambda$ = length constant of the gland, defined by: $\lambda = \sqrt{r_u/r_i}$

$l$ = the effective length of the distal part of the gland (*see* Discussion)

$l'$ = the morphological length of the gland

$L$ = $l/\lambda$

$M$ = number of cells abutting one cell

$N$ = the number of cells with equal order number

$p$ = the distance between the center of the ring of cells with order number $n$ and the center of the ring of cells with order number $n+1$. So: $p = d(1+\sin\varphi)$

$r$ = the radius of the lumen in the distal part

$R$ = the radius of the gland in the distal part

$r_i$ = the core resistance per unit length of gland

$r_L$ = the resistance of the membrane on the luminal side of the cells × unit length of gland

$r_M$ = the resistance of the membrane on the basal side of the cells × unit length of gland

$r_u$ = the nonjunctional membrane resistance × unit length of gland, defined by: $\frac{1}{r_u} = \frac{1}{r_M} + \frac{1}{r_L}$

$R_i$ = the resistance of the membrane between two cells with different order number (junctional resistance)

$R_L$ = the resistance of the membrane on the luminal side of a cell with order number $n$ ($n \geqq 1$)

$R_M$ = the resistance of the membrane on the basal side of a cell with order number $n$ ($n \geqq 1$)

$R_u$ = the resistance of the nonjunctional membrane of a cell with order number $n$ ($n \geqq 1$), defined by: $\frac{1}{R_u} = \frac{1}{R_L} + \frac{1}{R_M}$

$R_L^0$ = the resistance of the membrane on the luminal side of the most distal cell

$R_M^0$ = the resistance of the membrane on the basal side of the most distal cell (order number 0)

$S_i$ = the surface of the membrane between two cells with different order number

$S_L$ = the surface of the membrane on the luminal side of a cell with order number $n$ ($n \geqq 1$)

$S_M$ = the surface of the membrane on the basal side of a cell with order number $n$ ($n \geqq 1$)

$S_L^0$ = the surface of the membrane on the luminal side of the most distal cell

$S_M^0$ = the surface of the membrane on the basal side of the most distal cell

$t = \frac{1}{2}\alpha + \sqrt{(\frac{1}{2}\alpha)^2 - 1}$

$\tau$ = time after starting the current injection

$v_n$ = the voltage change in a cell with order number $n$

$v(x, \tau)$ = the induced potential

$x$ = the distance from the current electrode into the proximal direction along the gland axis

$X_1$ = the maximum length of the membrane on the basal side of cells with order number $n$ ($n \geqq 1$) in the axial direction (*see* Fig. 3*a*)

$X_2$ = the maximum length of these membranes in the perpendicular direction (*see* Fig. 3*a*).

*Discrete Models*

The discrete model descriptions are based upon the assumption that the resistance contribution of the cytoplasm may be neglected with regard to the junctional and the nonjunctional membrane resistances. Thus, the cells are equipotential spaces. Besides it will be assumed that the junctional resistances in the distal part are equal. The same is supposed for the nonjunctional resistances. If we assume that the junctional membranes have equal specific resistance and the same holds true for the nonjunctional membranes, this implies that all cells have the same shape and size.

*Configuration 1.* From observations it was found that the membranes on the basal side of the cells show a hexagonal pattern. Therefore, in the first model description the configuration of the cells in the distal part of the gland is supposed to be like that shown in Fig. 3*a*. Each cell has been given an order number $n$: the most distal cell has order number 0, the cells in the ring adjoining the most distal cell have order number 1, and so on. The shape of a cell with order number $n \geqq 1$ is shown in Fig. 3*b*. All cells are of the same shape and size. The membranes on the basal side of the cells have six sides with equal length $d$. Also the shapes of the membranes on the luminal side are mutually equal. An exception to the assumptions concerning the sizes is made for the most distal cell. The membrane on the basal and the luminal side of this cell have the form of half spheres with radius $R$ and $r$, respectively (*see* Fig. 3*a*).

In reality the shapes of the membranes are quite different from those shown in Fig. 3*b*, in which membrane foldings and microvilli are neglected.

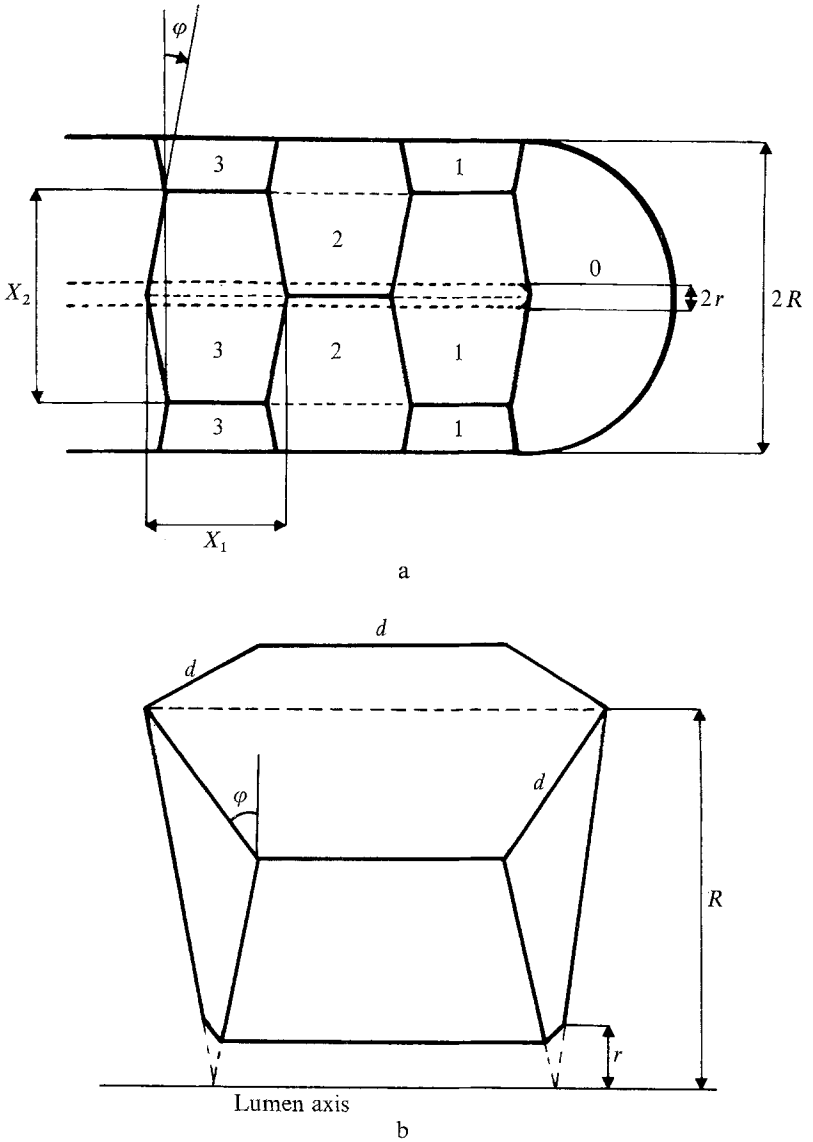


Fig. 3. (*a*) Model of configuration 1 of the cells in the distal part of the gland. Each cell has been given an order number. The radius of the lumen in this part of the gland is $r$ and the radius of the gland $R$. (*b*) Model of a cell with order number $n (n \geqq 1)$. Note that the distance from the lumen axis to all angular points of the hexagon representing the basal membrane are equal $R$. Similarly, the distances from the lumen axis to all angular points of the hexagon representing the luminal membrane are equal $r$

However, for the validity of the model with respect to the interpretation of experiments on cell communication, a morphological similarity is not required. It is only necessary that within reasonable limits the assumption concerning equalness of the permeabilities is satisfied.

Finally, it is supposed that the potentials within the bathing fluid and within the lumen are equal. This potential is taken as zero (*see* Discussion).

The relation between the order numbers and the potentials $v_n$ induced by the current injection $I$ in the most distal cell, is given by a set of difference equations obtained using Kirchhoff's current law:

$$\frac{2(v_{n-1}-v_n)}{R_i}=\frac{v_n}{R_L}+\frac{v_n}{R_M}+\frac{2(v_n-v_{n+1})}{R_i} \qquad (n\geqq 1)$$

with $R_L$, $R_M$ and $R_i$ the membrane resistances at luminal, basal and junctional sides of the cell, respectively. Using $\alpha=2+\frac{1}{2}\frac{R_i}{R_u}$ with $\frac{1}{R_u}$ denoting $\frac{1}{R_L}+\frac{1}{R_M}$ this equation simplifies to:

$$v_{n-1}+v_{n+1}=\alpha v_n \qquad (n\geqq 1). \tag{1}$$

By applying Kirchhoff's current law for the most distal cell (symbols referring to this cell are marked by the indices $_0$ or $^0$) one obtains:

$$IR_i=2N(v_0-v_1)+v_0\left(\frac{R_i}{R_M^0}+\frac{R_i}{R_L^0}\right). \tag{2}$$

The general solution of the second order difference Eq. (1) is given by:

$$v_n=c_1 t^n+c_2 t^{-n} \tag{3}$$

in which

$$t=\tfrac{1}{2}\alpha+\sqrt{(\tfrac{1}{2}\alpha)^2-1} \tag{4}$$

and $c_1$ and $c_2$ are constants.

If $v_n^{\exp}$ are the experimentally found values of the potentials in the different cells, the quantities $c_1$, $c_2$ and $t$ in Eq. (3) can be computed by applying the minimization procedure of Fletcher and Powell (1963) on the function:

$$G(c_1, c_2, t)=\sum_n (c_1 t^n+c_2 t^{-n}-v_n^{\exp})^2. \tag{5}$$

From the values of $c_1$, $c_2$ and $t$ the values for $v_0$, $v_1$ and so on can now be computed with Eq. (3). Also $\alpha$ can be computed from Eq. (4).

If $S$ denotes membrane surface, then $R_M^0/R_M=S_M/S_M^0$, $R_L^0/R_L=S_L/S_L^0$ and Eq. (2) changes into:

$$IR_i=2N(v_0-v_1)+v_0\cdot\frac{R_i}{R_u}\cdot\frac{S_L^0}{S_L}+v_0\cdot\frac{R_i}{R_M}\cdot\left\{\frac{S_M^0}{S_M}-\frac{S_L^0}{S_L}\right\}.$$

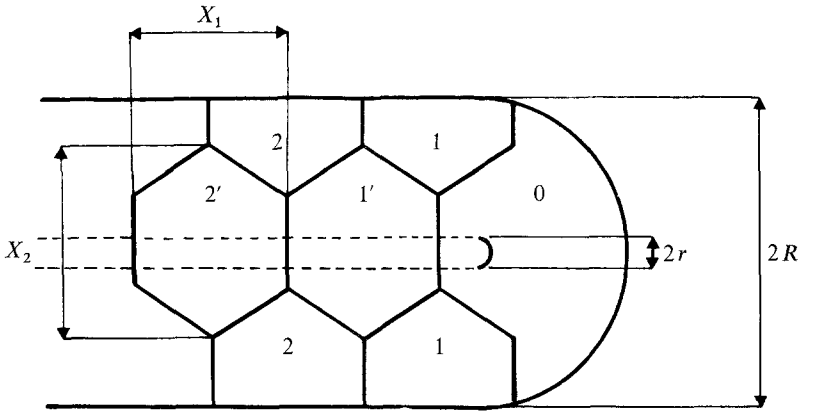


Fig. 4. Model of configuration 2 of the cells in the distal part of the gland. Two cell rows can be distinguished: in one row the cells have been given order numbers $n$ and in one row the cells have been given order numbers $n'$

Since $0 \leqq \frac{R_i}{R_M} \leqq \frac{R_i}{R_u} = 2(\alpha-2)$, the values of $R_i$ lie between

$$\frac{1}{I}\left\{2N(v_0-v_1)+v_0(\alpha-2)\cdot\frac{2S_L^0}{S_L}\right\} \quad \text{and} \quad \frac{1}{I}\left\{2N(v_0-v_1)+v_0(\alpha-2)\cdot\frac{2S_M^0}{S_M}\right\}. \quad (6)$$

$R_u$ can be computed from: $R_u = \frac{R_i}{2(\alpha-2)}$.

*Configuration 2.* It appears that the configuration of the cells in the gland sometimes shows a slightly different pattern as shown in Fig. 4. In this configuration two types of cell rows can be distinguished: type 1 in which the cells have order numbers $n$, and type 2 in which the cells have order numbers $n'$.

The condition that all cells have equal size and shape leads to a rather complex model of the unit cell. Therefore, the mathematical treatment will be omitted here and only a few results of the calculation are given in Fig. 5.

If we assume that both configurations are equally probable, it appears that in the average $(\alpha-2)$ must be 7% lower than calculated always using the equations of configuration 1. However, this correction will be partly cancelled by errors due to other approximations (*see* Discussion). Therefore we only used configuration 1 for the quantitative evaluation of cell coupling.

### *The Continuous Model*

Although the discrete model will be used for estimating $R_i$ and $R_u$, it is worthwhile to consider here also a continuous model in which the

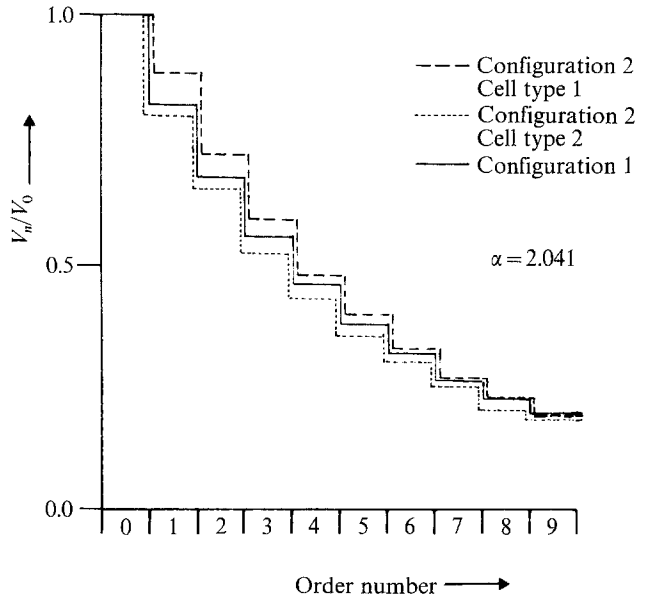


Fig. 5. The relationship between the order numbers and the potentials in the cells of configuration 1 and of the two types of cells of configuration 2 for $\alpha = 2.041$

junctional membrane resistances are included in the intracellular fluid resistance, while there exists no potential change in the radial direction within the gland. Such a model simplifies the interpretation of some results and is of interest for the comparison of our results with those of others. Finally, the evaluation of the time-dependent course of the induced potentials is rather complex using discrete models. The still elaborate mathematical treatment of this time course with the help of the continuous model following partly the theoretical approach of Hodgkin and Nakajima (1972) will be omitted here.

*Estimation of $r_u$ and $r_i$: Stationary Case.* It can easily be proved that the potential $v(x, \tau)$ must satisfy the following differential equation:

$$\lambda^2 \frac{\partial^2 v}{\partial x^2} - v = r_u c_u \frac{\partial v}{\partial \tau} \quad \text{(Cole, 1968).} \tag{7}$$

In the stationary case ($\partial v/\partial \tau = 0$) one obtains:

$$\lambda^2 \frac{\partial^2 v}{\partial x^2} = v. \tag{8}$$

The general solution of Eq. (8) is given by:

$$v(x) = c_1' \exp\left(\frac{x}{\lambda}\right) + c_2' \exp\left(-\frac{x}{\lambda}\right). \tag{9}$$

The general solution for the potentials using the first discrete configuration, given by Eq. (3) may also be written as:

$$v_n = c_1 \exp\left(\frac{n p \ln t}{p}\right) + c_2 \exp\left(-\frac{n p \ln t}{p}\right).$$

Taking $x = np$ this expression changes into:

$$v(x) = c_1 \exp\left(\frac{x \ln t}{p}\right) + c_2 \exp\left(-\frac{x \ln t}{p}\right).$$

From this expression and Eq. (9) it follows that:

$$\begin{aligned} \lambda &= p/\ln t \\ c_1' &= c_1 \\ c_2' &= c_2. \end{aligned} \tag{10}$$

Thus, essential parameters of the continuous model can be calculated from the results obtained by applying the discrete model.

Also $r_i$ and $r_u$ can be computed from the values of $R_i$ and $R_u$ obtained from the experimental results using the discrete configuration 1 by applying the following procedure: In the honeycomb structure of the first discrete configuration of the salivary gland a repeating rectangular unit can be found (*see* Fig. 6). The resistance of such a unit in the axial direction of the gland is given by: $\frac{1}{2} \cdot 2 \cdot R_i$. So the core resistance $r_i$ per unit length of the gland is given by:

$$r_i = \frac{R_i}{2 \cdot N \cdot p}. \tag{11}$$

In the same way the nonjunctional resistance of a unit length of the gland can be calculated:

$$r_u = \frac{R_u \cdot p}{N}. \tag{12}$$

## Results

### *Morphological Properties*

To illustrate that the cells of the gland show a hexagonal pattern, we chose from each of the 68 glands studied a cell where its neighbor cells showed up rather well. The number $M$ of abutting cells was counted. A frequency distribution of the results is shown in Fig. 7*A*. The distribution shows a clear peak for $M = 6$ (mean 5.8).

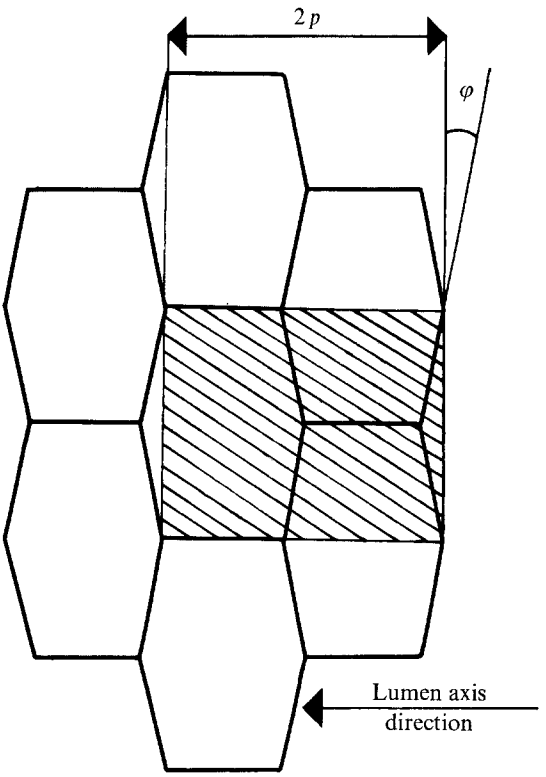


Fig. 6. Part of the honeycomb structure of the gland in which a repeating rectangular unit can be distinguished

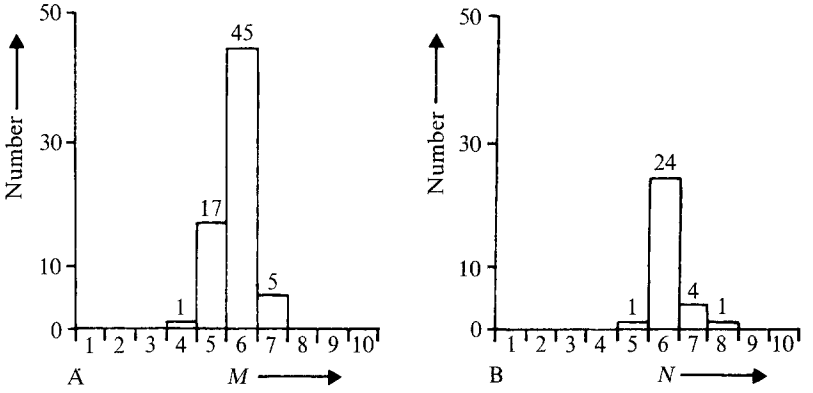


Fig. 7. (*A*) Frequency histogram of the cells in the distal part of the gland with respect to the number of their neighbors. (*B*) Frequency histogram of the number of cells in the distal part with equal order number

Table 1. Morphological properties of the salivary glands

| Quantity | Age: 145 to 155 hr | | | Age: 155 to 165 hr | | |
|---|---|---|---|---|---|---|
| | Averaged value | SD | No. of measurements | Averaged value | SD | No. of measurements |
| $M$ | (5.8) | | (68) | 5.8 | | 68 |
| $N$ | (6.2) | | (30) | 6.2 | | 30 |
| $R$ | 90 μm | 20 μm | 10 | 110 μm | 10 μm | 30 |
| $r$ | 10 μm | 3 μm | 10 | 8 μm | 2 μm | 30 |
| $X_1/X_2$ | (0.74) | | (30) | 0.74 | 0.12 | 30 |
| $l'$ | 1260 μm | 200 μm | 10 | 1600 μm | 200 μm | 30 |

Table 2. Computed quantities in the model of the cells of the salivary glands

| Quantity | Age: 145 to 155 hr | Age: 155 to 165 hr |
|---|---|---|
| $\sin(\varphi)$ | 0.22 | 0.22 |
| $d$ | 49 μm | 58 μm |
| $p$ | 60 μm | 70 μm |
| $S_M$ | 5,800 μm² | 7,900 μm² |
| $S_L$ | 610 μm² | 570 μm² |
| $S_M^0$ | 51,000 μm² | 76,000 μm² |
| $S_L^0$ | 620 μm² | 400 μm² |
| $S_i$ | 2,100 μm² | 3,200 μm² |

From 30 of these salivary glands some morphological properties (Table 1) and the frequency distribution of the number $N$ of cells with equal order number situated in a ring were estimated. The distribution of $N$ is given in Fig. 7*B* and shows a sharp peak for $N = 6$ (mean 6.2).

The salivary glands with an age of 145 to 155 hr have the same form as the salivary glands with an age of 155 to 165 hr. The values of $M$, $N$ and $X_1/X_2$ of the younger glands do not change significantly during this period. Using the values of Table 1 a number of quantities in the model of the cells of the gland can be computed. They are listed in Table 2.

### *Electrical Measurements*

The measurements of the electrical coupling were carried out by injecting a 1-Hz symmetrical square wave with an amplitude of 10 nA into the most distal cell. Measurements with amplitudes up to 40 nA show a linear relationship between the voltage changes on different locations and the amplitude of the injected current.

Table 3. Results obtained from 10 salivary glands with an age of 145 to 155 hr

| | $\alpha$ | $\lambda$[a] (mm) | $R_i$ (MΩ) | $R_u$ (MΩ) | $\frac{c_1}{c_2}$ | $c_u$ (μF/mm) |
|---|---|---|---|---|---|---|
| Averaged value | 2.012 | 0.64 | 0.23 | 11 | 0.18 | 0.28 |
| SD | 0.008 | 0.20 | 0.12 | 3 | 0.13 | 0.06 |
| Range | | | | | | |
| min. | 2.003 | 0.35 | 0.08 | 7.3 | −0.04 | 0.21 |
| max. | 2.029 | 1.06 | 0.42 | 16 | 0.28 | 0.38 |

[a] Each parameter value in the top row of the Table is the mean of the values computed separately for each of the 10 glands. Thus, the top listed value of $\lambda$ was calculated by averaging the values of $\lambda$ found for every gland by means of Eq. (10).

Table 4. Results obtained from 27 salivary glands with an age of 155 to 165 hr

| | $\alpha$ | $\lambda$ (mm) | $R_i$ (MΩ) | $R_u$ (MΩ) | $\frac{c_1}{c_2}$ | $c_u$ (μF/mm) |
|---|---|---|---|---|---|---|
| Averaged value | 2.030 | 0.53 | 0.37 | 9.6 | 0.04 | 0.21 |
| SD | 0.020 | 0.23 | 0.22 | 5.5 | 0.06 | 0.10 |
| Range | | | | | | |
| min. | 2.006 | 0.25 | 0.10 | 2.4 | −0.11 | 0.09 |
| max. | 2.080 | 1.20 | 1.00 | 20 | 0.21 | 0.42 |

In Tables 3 and 4 the results of the measurements on the electrical coupling are given. The values of $R_i$ in Tables 3 and 4 were calculated as the averaged value of the two values of Eq. (6). In these Tables all but the last column are based on the discrete model.

Fig. 8 shows a typical result of the measurements on a salivary gland with an age of 155 to 165 hr. The parameters of the best fitting theoretical curve in Fig. 8 are: $\alpha = 2.041$; $c_1 = 0.06$ mV and $c_2 = 1.86$ mV.

*The Change of the Parameters $R_i$, $R_u$ and $c_u$ Induced by Lysolecithin*

The model descriptions were applied among others to investigate the influence of lysolecithin on the electrical cell coupling. First the parameters were estimated from measurements on a salivary gland (155 to 165 hr) in the normal medium. Then this salivary gland was transferred to medium containing lysolecithin, 1-palmitoyl-*sn*-glycero-3-phosphorylcholine (90 μg/ml) and the measurements were repeated after half an hour. To check the reversibility of the process the salivary gland was replaced in the normal medium and the measurements were carried out again. The results of such

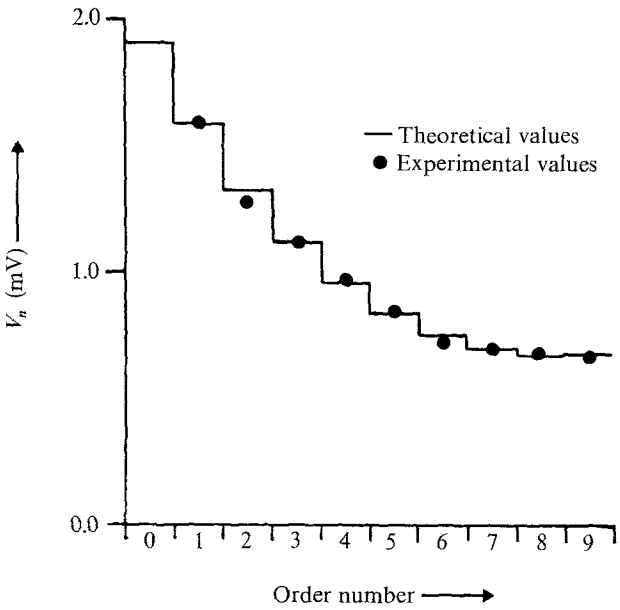


Fig. 8. Typical result of the measurement on electrical coupling in a gland with age between 155 and 165 hr. The drawn line represents the best fitting curve and the circles represent the experimentally found values

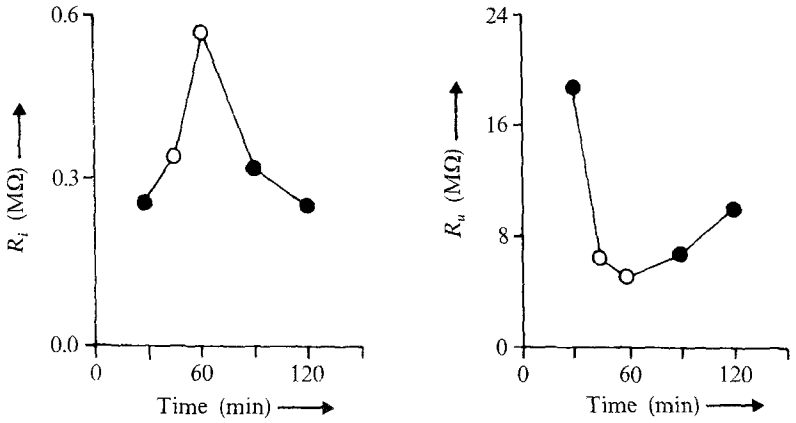


Fig. 9. Typical result of measurements on the influence of lysolecithin upon $R_i$ and $R_u$. The open circles are values of $R_i$ and $R_u$ estimated from measurements in lysolecithin-containing medium; the dark circles are values of $R_i$ and $R_u$ of the same gland in normal medium

measurements on nine glands are listed in Table 5, whereas a typical result is shown in Fig. 9. For the computations, the averaged values from Tables 1 and 2 were used (*see also* Discussion).

Table 5. Results of experiments concerning the influence of lysolecithin on electrical cell coupling

| | $R_i^{lys}$ (MΩ) | $R_i^{norm}$ (MΩ) | $R_i^{lys}/R_i^{norm}$ | $R_u^{lys}$ (MΩ) | $R_u^{norm}$ (MΩ) | $R_u^{lys}/R_u^{norm}$ |
|---|---|---|---|---|---|---|
| | 0.43 | 0.22 | 2.0 | 2.7 | 7.9 | 0.34 |
| | 0.82 | 0.52 | 1.6 | 4.1 | 12.5 | 0.33 |
| | 0.46 | 0.28 | 1.6 | 5.7 | 12.0 | 0.48 |
| | 0.31 | 0.29 | 1.1 | 7.2 | 13.0 | 0.55 |
| | 0.60 | 0.36 | 1.7 | 6.0 | 4.2 | 1.43 |
| | 0.12 | 0.23 | 0.5 | 4.1 | 7.3 | 0.56 |
| | 0.64 | 0.40 | 1.6 | 7.9 | 9.7 | 0.81 |
| | 0.92 | 0.24 | 3.8 | 4.4 | 14.0 | 0.31 |
| | 0.85 | 0.32 | 2.4 | 6.3 | 7.9 | 0.80 |
| | — | — | — | — | — | — |
| Averaged value | 0.57 | 0.32 | 1.8 | 5.4 | 9.8 | 0.62 |
| SE | | | 0.3 | | | 0.10 |

$R_i^{lys}$ and $R_u^{lys}$ denote the values of the junctional and the nonjunctional membrane, respectively, in lysolecithin-containing medium. $R_i^{norm}$ and $R_u^{norm}$ are the values of these membranes in normal medium. Also the averaged values and the standard errors of the ratios are given.

Lysophosphatidyl choline (lyso PC) induces a decrease of the nonjunctional resistance and an increase of the junctional resistance. (However, in one gland $R_i$ decreased and in another one $R_u$ increased.) The increased permeability of the nonjunctional membrane is not surprising as van Zutphen (1970) and Reman (1971) demonstrated that lyso PC was able to influence the membrane permeability in that way. The decreased permeability of the low resistance junction parallel, and probably consequent to the increased nonjunctional permeability (and membrane potential) agrees with uncoupling experiments described earlier in the literature (Loewenstein, 1966; Loewenstein, Nakas & Socolar, 1967; Oliveira-Castro & Loewenstein, 1971; Socolar & Politoff, 1971). There was no significant change in the capacity of the nonjunctional membrane during the experiments.

It is notable, furthermore, that the glands were easier to impale when incubated in the medium containing lyso PC. This may be due to the fact that the mechanical stability of the nonjunctional membrane is reduced. Possibly the same mechanism is responsible for the increase in permeability as for the reduction of the mechanical stability of the nonjunctional membrane.

Finally, it should be mentioned that there was a reversible decrease of about 20% in the intracellular potential of the gland cells during incubation

in the lysolecithin-containing medium. This may be caused by the increase of the permeability of the nonjunctional membrane. It also agrees with observations that there exists a parallelism between the membrane potential and the extent of intracellular communication (Rose, 1970).

### *Change of Coupling with Age*

If we compare the results between the younger and the older glands it may be concluded that although there is an overlap between the values of $R_i$, the difference in the average is significant. From the values of $S_i$ (Table 2) it follows that this cannot be due to the difference in projected surface of the junctional membrane. The values of $R_u$ and $c_u$ cannot be compared because of the fact that the ratio between the surfaces $S_M$ and the ratio between the surfaces $S_L$ are not equal. In any case, Tables 3 and 4 show no significant difference between the $R_u$ values in younger and older glands.

The finding of a higher coupling in younger glands agrees with the measurements of Loewenstein and Kanno (1964) on the salivary gland of larvae in the early or midstages of the third instar period. Our measurements were done on salivary glands of larvae in the end of the third instar. As may be expected we found values for $R_i$ which are higher than those found by Loewenstein and Kanno. A decrease in coupling with age was also shown for *Chironomus* salivary gland (Loewenstein, Socolar, Higashino, Kanno & Davidson, 1965).

It is not sensible to calculate specific membrane resistances, because of the fact that the membrane foldings on the basal side of the cell are quite different from the membrane foldings on the luminal side, and because of the fact that the morphological shape of the cells will not be exactly equal to the shape of the postulated unit cell.

## Discussion of the Model Descriptions

### *The Reliability Criterion*

Only those series for which the number of measured orders $J$ was greater than or equal to 6 were used for the evaluation:

$$J \geqq 6. \tag{13a}$$

It is possible to measure the potentials with an accuracy of about 0.1 to 0.15 mV. Therefore, only those series for which

$$\frac{1}{J-3} G = \frac{1}{J-3} \sum_{n=1}^{J} (v_n^{\text{exp}} - v_n^{\text{theor}})^2 \leqq 0.015 \text{ (mV)}^2 \tag{13b}$$

were used in Tables 3, 4 and 5 ($J-3$ is the number of degrees of freedom in the fitting procedure). We will call this pair of conditions the reliability criterion.

*The Accuracy of the Estimated Values*

(*a*) The reliability criterion is a condition of data collection that sets bounds on errors. To get an impression about the errors in the estimated values of $R_i$ and $R_u$ bounded by this criterion, the following procedure was carried out: For the parameters $c_1$, $c_2$ and $\alpha$ five different values covering the range of experimentally found values were taken: namely $c_1$, respectively, $-0.2$, $-0.1$, 0.1, 0.3, 0.5 mV; $c_2$, respectively, 1.5, 1.75, 2.0, 2.25, 2.5 mV; and $\alpha$, respectively, 2.001, 2.005, 2.02, 2.05, 2.10. In this way $5 \times 5 \times 5 = 125$ different sets ($c_1$, $c_2$, $\alpha$) are obtained. For each set the potentials $v_1$, $v_2$, ... $v_9$ ($J = 9$) were calculated with the aid of Eq. (3). Those sets giving rise to physically impossible potential distributions (potential not monotonously decreasing with increasing order number or including negative values) were omitted. For different values of $c_1^*$ around $c_1$, $c_2^*$ around $c_2$, $\alpha^*$ around $\alpha$, the value of

$$G = \sum_{n=1}^{9} \left(v_n(c_1^*, c_2^*, \alpha^*) - v_n(c_1, c_2, \alpha)\right)^2$$

was calculated. From the results of these calculations it could be concluded that under the most unfavorable condition [$G = 6 \times 0.015 = 0.09$ (mV)$^2$], and if the errors in the potential measurements are systematic, the maximum deviation between $R_i$ and $R_u$ as computed from ($c_1$, $c_2$, $\alpha$) and as computed from ($c_1^*$, $c_2^*$, $\alpha^*$) varies between 10 and 40 %. The series evaluated in Tables 3, 4 and 5 show an average value $G \approx 0.04$ (mV)$^2$. In that case the deviation in $R_i$ and $R_u$ varies between 5 and 20 %. Since part of the errors in the potential measurements are certainly not of a systematic character, the average inaccuracy in $R_i$ and $R_u$ is not likely to exceed 10 %. The same results are found in cases of the other values of $J$ (6, 7, 8).

(*b*) The errors in the morphological quantities in Tables 1 and 2 may introduce errors in $R_i$ and $R_u$ in the order of 20 %. In the case that measurements on one gland are compared, the errors in the morphological quantities are not important because they influence the results of the measurements on that gland always in the same way!

(*c*) A possibly important source of systematic error arises from the fact that $R_i$ is approximated as the arithmetic mean of an underestimate and an overestimate [Eq. (6)]. This may maximally introduce an error in $R_i$ of half of the difference between these estimates being about 10 % and accordingly the same error in $R_u$.

The question may arise, in a case where $R_i$ really does not, for example, increase, is it possible that changes can occur in nonjunctional resistance values in such a way as to give an exaggerated overestimation of $R_i$ in the final state? To investigate this possibility we chose a fixed value for $R_i$ and $R_L$ and calculated three series $v_1$, $v_2$, ... $v_9$ for $R_M$, respectively, equal to $2R_L$, $R_L$, $\frac{1}{2}R_L$, assuming a gland length of 10 cells. The same was done for fixed values of $R_i$, $R_M$ and $R_L$, respectively, equal to $2R_M$, $R_M$, $\frac{1}{2}R_M$. This procedure was carried out for values of $\alpha$, respectively, 2.001, 2.005, 2.02, 2.05, 2.10. From the constructed series $R_i$ was calculated using the minimization procedure and Eq. (6). The results show that an increase of $R_L$ with a factor 2 produces a very small artificial decrease of the estimate of $R_i$ of less than 1%. Furthermore, an increase of $R_M$ with a factor 2 produces an artificial increase of the estimate of $R_i$ of maximally 5%. Thus, in any case, changes of $R_i$ and $R_u$ in opposite directions can not very well be due to the averaging procedure mentioned [Eq. (6)].

*In summary*: If the errors combine in a manner usually supposed for random errors, the inaccuracy in $R_i$ and $R_u$ for one gland in Tables 3 and 4 will be equal to the square root of the summed error squares, which is equal to 25%. For conclusions based upon Table 5 only the errors in $R_i$ and $R_u$ of 10% described in part (*a*) are important.

### *The Effective Length of the Gland*

Because of the finiteness of the distal part of the gland, there must be a value $l$ for $x$ at which the potential satisfies the condition:

$$\left(\frac{\partial V}{\partial x}\right)_{x=l} = 0.$$

This value of $x$ will be defined as the effective length $l$.

If the salivary gland would be a core with uniform composition the quantity $l$ would be equal to the morphological length $l'$.

Berendes (1965) describes cell properties of the gland in relation to development and showed that the proximal cells differ distinctly from the distal cells during the third instar. The cells in the distal part of the gland are much larger than those in the proximal part. Also the cytoplasmic content of the distal cells differs from that of the proximal cells. Under phase contrast as well as in sectioned material, a sharply defined boundary between both cell types can be seen. This boundary is moving from distal to

proximal during the third instar, whereas the total number of cells per gland remains constant.

Thus, the salivary glands used in our experiments are not cores with uniform composition. However, between 145 and 165 hr the distal part of the salivary gland shows a uniform composition. So the induced stationary potentials in this part are given by Eqs. (3) or (9).

The effective length $l$ of the distal part equals: $l=\frac{\lambda}{2}\ln\left(\frac{c_2}{c_1}\right)$ or: $L=\frac{1}{2}\ln\left(\frac{c_2}{c_1}\right)$, $L$ being the normalized effective length.

From Tables 3 and 4, however, it follows that the SD of $c_1/c_2$ is relatively high. So it is to be expected that the individual values of $c_1/c_2$ show a high inaccuracy (even some values are negative). It seemed reasonable to us to use the averaged value of $c_1/c_2$ as a more appropriate value for the estimation of a mean value of $L$. From this value it follows that for salivary glands with an age of 155 to 165 hr the value of $L$ is $L=1.6$. For the younger glands this value is $L=0.85$. Then the averaged effective length $l=L\cdot\lambda$) of the older glands is 850 $\mu$m, whereas the morphological length $l'$ is about 1600$\mu$m. For the younger glands these values are 550 and 1260 $\mu$m, respectively.

The fact that $l$ is much smaller than $l'$ is also illustrated in Fig. 8. In this case the effective length is only about 600 $\mu$m (9th order). The curve in Fig. 5 shows the course of the potential as a function of the order numbers with the same value for $\alpha$ as in Fig. 8, but for an effective length of 1600 $\mu$m.

The fact that $l/l'$ of the older glands seems to have a somewhat higher value than $l/l'$ of the younger glands can be understood from the fact that the boundary between the cells with different properties is moving from distal to proximal during the development.

During the experiments it was observed that on the average the boundary between the cells with different properties lies at about 650 $\mu$m in the older glands.

If we assume that the older salivary gland consists of a distal compartment (morphological length 650 $\mu$m) and a proximal compartment (morphological length 950 $\mu$m) a relation between the core resistance $r_i^p$ and the nonjunctional resistance $r_u^p$ of the proximal part can be estimated using the following procedure: Using Eqs. (9) and (10) and the values of Table 4 the potential $V_p$ at the boundary between the proximal and the distal part together with the current $I_p$ entering from the distal compartment into the proximal one can be calculated as a function of $c_2$. Because the potential in the proximal part must satisfy Eq. (9) it can be shown that the relation between the core resistance $r_i^p$ and the nonjunctional resistance $r_u^p$ of the

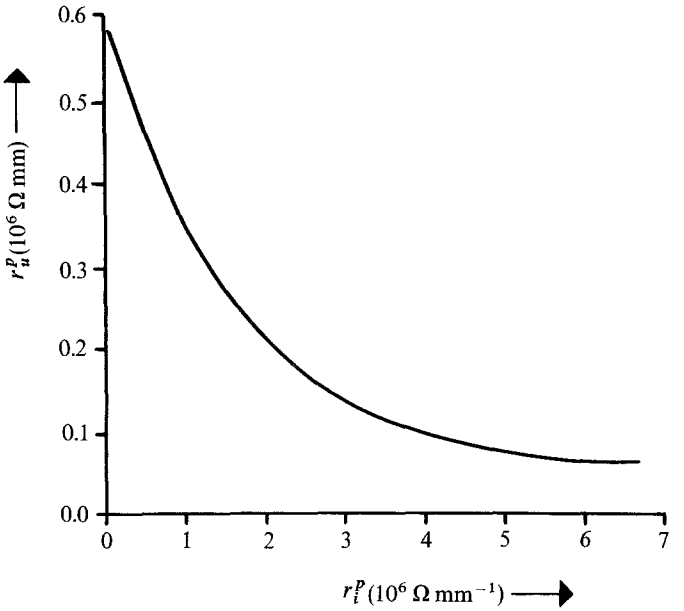


Fig. 10. Relation between the core resistance $r_i^p$ and the nonjunctional resistance $r_u^p$ of the proximal part. The curve represents the combinations of $r_i^p$ and $r_u^p$ which satisfy the relation:

$$\sqrt{r_u^p r_i^p} = \frac{V_p}{I_p} \operatorname{tgh}\left(\frac{l^p}{\sqrt{\frac{r_u^p}{r_i^p}}}\right) \quad \text{with } l^p = 950\ \mu\mathrm{m}$$

proximal part is given by:

$$\sqrt{r_u^p \cdot r_i^p} = \frac{V_p}{I_p} \operatorname{tgh}\left(l^p \sqrt{\frac{r_i^p}{r_u^p}}\right) \quad \text{with } l^p = 950\ \mu\mathrm{m}.$$

The curve in Fig. 10 shows the combinations of $r_i^p$ and $r_u^p$ which satisfy this condition.

For the distal part it was found, using Eqs. (11) and (12), that $r_i = 0.43\ \mathrm{M}\Omega\,\mathrm{mm}$ and $r_u = 0.11\ \mathrm{M}\Omega\,\mathrm{mm}$; this combination differs significantly from the combinations in Fig. 10. This suggests a difference between the parameters of the proximal part and the parameters of the distal part.

### *The Potential Changes in the Lumen*

All calculations are carried out under the assumption that the potential change in the lumen is zero. To check this assumption in 10 cases this potential was measured. After impaling a neighbor cell of the most distal

cell the micropipette was carefully inserted into the lumen. This was attended with a sudden drop in potential to about 0 mV. After that a current with an amplitude of 10 nA was injected into the most distal cell. The induced potential $V_L$ in the lumen was on the average 0.08 mV, whereas the value of the induced potentials in the cell with order number 1 was about 2 mV.

To get an impression about the influence of a nonzero potential in the lumen an averaged series was constructed from all series of the older glands. From this series $\alpha$ was estimated. After subtraction of $V_L$ from the values of $v_n$ a new $\alpha^*$ was calculated. It was found that $(\alpha^* - 2)$ is about 7% higher than $(\alpha - 2)$. However, this error will be partly compensated by the fact that only configuration 1 of the discrete model was used. This will lower the value of $\alpha$ again by about 7%, as mentioned before.

### *Comparison of the Models*

Our previous discussions and definitions of $R_i$ and $r_i$ consider only junctional resistance contributions, but the experimental values of $R_i$ and $r_i$ in the Tables and the Figures obviously include cytoplasmatic contributions too.

If the cytoplasmic resistance contribution is not neglected, the resistance $r_a$ per unit length in the axial direction is given by [*see* Fig. 6 and Eq. (11)]

$$r_a = r_i + \frac{\rho_c}{\pi(R^2 - r^2)}$$

in which $\rho_c$ is the cytoplasmic resistance which is of the order of $10^3$ $\Omega$mm (Schanne, 1969).

Using the values listed in Tables 1–4 it follows that for the older glands the resistance contribution of the cytoplasm is about 5% of the resistance contribution of the junctional membrane. For the younger glands this value is about 10%. This means that in both cases the discrete model is the most realistic model of the gland.

If the effective length of the gland would be equal to the morphological length, the continuous treatment as done by Loewenstein and Kanno (1964) would be simpler than the discrete one. Because of the difference between the proximal and distal part of our object, the effective length is not known and can only be estimated by minimization procedures using Eq. (9). Thus, the continuous model is not preferable to the discrete one in order to calculate membrane resistances. The function in Eq. (9) is similar to the function describing potentials in the discrete model [*see* Eq. (10)].

Moreover, the discrete presentation is simpler concerning the numerical treatment. Furthermore, the estimation of order number is easier than the measuring of distances.

Our thanks are due to Mrs. Karin Hogema for her skillful technical assistance. We wish to thank Dr. P. F. Elbers (Biological Ultrastructure Research Unit, Utrecht), Dr. H. J. Leenders (Cell Biology Section, University of Nijmegen) and Dr. J. Siegenbeek van Heukelom (Department of Animal Physiology, University of Amsterdam) for useful comments. Furthermore, we wish to thank Dr. J. A. J. Faber (Mathematical Institute, Department of Statistics, University of Utrecht) and Dr. H. van der Vorst (Academical Computer Centre, Utrecht) for useful discussions.

## References

Berendes, H. D. 1965. Salivary gland function and chromosomal puffing patterns in *Drosophila hydei*. *Chromosoma (Berl.)* **17**:35

Cole, K. S. 1968. Membranes, ions and impulses. A chapter of classical biophysics. *In:* Biophysics Series. Cornelius A. Tobias, editor. p. 66. University of California Press, Berkeley and Los Angeles

Fletcher, R., Powell, M. J. D. 1963. A rapidly convergent descent method for minimization. *Computer J.* **6**:163

Furshpan, E. J., Potter, D. D. 1968. Low resistance junctions between cells in embryos and tissue culture. *Curr. Top. Devel. Biol.* **3**:95

Hax, W. M. A., van Venrooij, G. E. P. M., Vossenberg, J. B. J. 1974. Cell communication—A cyclic-AMP mediated phenomenon. *J. Membrane Biol.* **19**:253

Hodgkin, A. L., Nakajima, S. 1972. The effect of diameter on the electrical constants of frog skeletal muscle fibres. *J. Physiol.* **221**:105

Loewenstein, W. R. 1966. Permeability of membrane junctions. *Ann. N.Y. Acad. Sci.* **137**:441

Loewenstein, W. R. 1968. Communication through cell junctions. Implications in growth control and differentiation. *Devel. Biol.* **19** (suppl. 2):151

Loewenstein, W. R., Kanno, Y. 1964. Studies on an epithelial (gland) cell junction. I. Modifications of surface membrane permeability. *J. Cell Biol.* **22**:565

Loewenstein, W. R., Nakas, M., Socolar, S. J. 1967. Junctional membrane uncoupling. Permeability transformations at a cell membrane junction. *J. Gen. Physiol.* **50**:1865

Loewenstein, W. R., Socolar, S. J., Higashino, S., Kanno, Y., Davidson, N. 1965. Intercellular communication: Renal, urinary bladder, sensory and salivary glands. *Science* **149**:295

Oliveira-Castro, G. M., Loewenstein, W. R. 1971. Junctional membrane permeability. Effects of divalent cations. *J. Membrane Biol.* **5**:51

Poels, C. L. M. 1970. Time sequence in the expression of various developmental characters induced by Ecdysterone in *Drosophila hydei*. *Devel. Biol.* **23**:210

Poels, C. L. M. 1972. Mucopolysaccharide secretion from *Drosophila* salivary gland cells as a consequence of hormone induced gene activity. *Cell Diff.* **1**:63

Reman, F. C. 1971. Interaction of Synthetic Lecithins and Lysolecithins with Erythrocytes and Oriented Lipid Structures. Ph. D. Thesis. University of Utrecht, Utrecht, The Netherlands

Rose, B. 1970. Junctional membrane permeability; restoration by a repolarizing current. *Science* **169**:607

Schanne, O. F. 1969. Measurement of cytoplasmic resistivity by means of the glass microelectrode. *In:* Glass Microelectrodes. M. Lavallée, O. F. Schanne and N. C. Hébert, editors. p. 299. J. Wiley and Sons, Inc., New York

Siegenbeek van Heukelom, J., Denier van der Gon, J. J., Prop, F. J. A. 1970. Epithelial monolayers: A study object for cell communication. *Biochim. Biophys. Acta* **211**:98

Siegenbeek van Heukelom, J., Denier van der Gon, J. J., Prop, F. J. A. 1972. Model approaches for evaluation of cell coupling in monolayers. *J. Membrane Biol.* **7**:88

Siegenbeek van Heukelom, J., Slaaf, D. W., van der Leun, J. C. 1972. Cell communication in the basal cells of the human epidermis. *Biophys. J.* **12**:1266

Socolar, S. J., Politoff, A. L. 1971. Uncoupling cell junctions in a glandular epithelium by depolarizing current. *Science* **172**:492

van Zutphen, H. 1970. Effects of Polyene Antibiotics, Vitamin D, and Lysolecithins on Lipid Bilayer Membranes. Ph. D. Thesis. University of Utrecht, Utrecht, The Netherlands